Title
Control of Arabidopsis apical-basal embryo polarity by antagonistic transcription factors.

Journal
Nature, 464(7287)

ISSN
0028-0836

Authors
Smith, Zachery R
Long, Jeff A

Publication Date
2010-03-01

DOI
10.1038/nature08843

Peer reviewed

HHS Public Access

Author manuscript

Nature. Author manuscript; available in PMC 2010 September 18.

Published in final edited form as:

Nature. 2010 March 18; 464(7287): 423–426. doi:10.1038/nature08843.

Control of Arabidopsis apical-basal embryo polarity by antagonistic transcription factors

Zachery R. Smith[1,2] and **Jeff A. Long**[1]

[1]Plant Biology Laboratory, The Salk Institute for Biological Studies, University of California San Diego, La Jolla, California 92037, USA

[2]Department of Biology, La Jolla, California 92037, USA

Abstract

Plants, similar to animals, form polarized axes during embryogenesis upon which cell differentiation and organ patterning programs are orchestrated. During *Arabidopsis* embryogenesis, establishment of the shoot and root stem cell populations occurs at opposite ends of an apical-basal axis. Recent work has identified the *PLETHORA* (*PLT*) genes as master regulators of basal/root fate1–3, while the master regulators of apical/shoot fate have remained elusive. Here we show that the *PLT1* and *PLT2* genes are direct targets of the transcriptional corepressor *TOPLESS* (*TPL*) and that *PLT1/2* are necessary for the homeotic conversion of shoots to roots in *tpl-1* mutants. Using *tpl-1* as a genetic tool, we identify the *CLASS III HOMEODOMAIN-LEUCINE ZIPPER* (*HD-ZIP III*) transcription factors as master regulators of embryonic apical fate, and show they are sufficient to drive the conversion of the embryonic root pole into a second shoot pole. Furthermore, genetic and misexpression studies reveal an antagonistic relationship between the *PLT* and *HD-ZIP III* genes in specifying the root and shoot pole.

During early embryogenesis, the phytohormone auxin plays a critical role in apical-basal axis formation4. Auxin-induced gene expression involves degradation of AUX/IAA transcriptional repressors5, and *IAA12/BODENLOS* was shown to require the transcriptional co-repressor *TOPLESS* (*TPL*) for its function during embryonic root development6. In the dominant negative *tpl-1* allele the embryonic shoot pole is transformed into a second root pole (Fig. 1a, b), indicating that root specifying genes must be actively repressed in the apical half of the embryo for normal apical/basal patterning7,8. *tpl-1* is temperature sensitive and shows a high frequency of shoot to root transformation when embryos develop at 29°C8. In wild-type (WT) plants, *PLT1* and *PLT2* are expressed in the root meristem throughout embryo development1 (Fig. 1d, f). In *tpl-1* grown at 29°C, both *PLT1* and *PLT2* are misexpressed in the apical domain, beginning at the heart stage (Fig. 1e, g). It has been

Correspondence and requests for materials should be addressed to J.A.L. (long@salk.edu).

Author Contributions Z.R.S. collected the data. Z.R.S. and J.A.L. designed the study and wrote the manuscript.

The authors declare no competing financial interests.

shown that the *PLT* genes are sufficient to initiate ectopic roots when driven from an embryonic promoter1, suggesting that the misexpression seen in *tpl-1* is causative of the double root phenotype. In agreement with this, double root formation was never observed in *tpl-1 plt1-5 plt2-1* embryos grown at 29°C (n>1000) (Fig. 1c). Thus, the *PLT* genes are necessary for apical root formation in *tpl-1*. To assess whether the *PLT* genes are direct targets of TPL repression, we performed Chromatin Immunoprecipitation (ChIP) on *TPLp::TPL-HA* dissected ovules containing globular to heart stage embryos. We observed enrichment of regions in both the *PLT1* and *PLT2* promoters in the TPL ChIP samples (Fig. 1h, i), indicating that TPL acts in the apical region of the embryo by directly repressing *PLT* expression.

A second-site modifier screen on *tpl-1* uncovered a semi-dominant mutant that completely suppressed the formation of double-root seedlings (Supplementary Fig. 2). Map-based cloning identified a single mis-sense mutation within the *HD-ZIP III* transcription factor *PHABULOSA* (*PHB*) in this mutant, which we designate *phb-14d*. This mutation resides within a known *microRNA (miR)165/166* family binding site and is predicted to result in a loss of *miR165/166* mediated regulation9,10. Notably, the observed increase in *PHB* transcript abundance is less severe than previously described alleles (Supplementary Fig. 2).

All five *HD-ZIP III* genes (*PHB*, *PHAVOLUTA* (*PHV*), *REVOLUTA* (*REV*), *INCURVATA4*/*CORONA* (*ICU4/CNA*), and *ARABIDOPSIS THALIANA HOMEOBOX-8* (*ATHB-8*)) are predicted to be regulated by *miR 165/166*9–12. Semi-dominant gain-of-function (GOF) mutations in the miR binding site of *PHB*, *PHV*, *REV*, and *ICU4* have been previously characterized for their role in specifying adaxial/dorsal fate in lateral organs and vasculature11,13–16. Although neither *rev-10d* nor *icu4-1d* display obvious embryonic patterning defects (Supplementary Fig. 2), they also completely suppress the shoot to root transformation seen in *tpl-1* when grown at 29°C (n>1000) (Supplementary Fig. 2). These results suggest that the *HD-ZIP III* genes play an important role in promoting apical fate in early embryogenesis.

Consistent with the observation that the GOF mutations in *HD-ZIP III* genes restore apical fate to *tpl-1* embryos, *PHB*, *PHV*, *REV*, and *ICU4* are all expressed in an apical/central domain of the globular embryo17 (Fig. 2a, Supplementary Fig. 3). By the heart stage, the expression of all four genes expands to the adaxial domain of the cotyledons and throughout the provascular tissue17 (Fig. 2b, Supplementary Fig. 3). In *tpl-1* embryos grown at 29°C, *PHB*, *PHV*, *REV*, and *ICU4* expression is identical to WT at the globular stage, but is absent from the apical domain by the heart stage (Fig. 2c, Supplementary Fig. 3). Persistent *PHB* expression in the apical domain in *tpl-1 phb-14d* embryos grown at 29°C (Fig. 2d) suggests that increasing *HD-ZIP III* transcript abundance is sufficient to restore apical fate in *tpl-1*.

We then examined the radial organization of the apical domain of these embryos at 29°C by determining the expression patterns of the *FILAMENTOUS FLOWER* (*FIL*) and *WUSCHEL* (*WUS*) genes. *FIL* is normally expressed peripheral to the meristem in globular stage WT embryos (Supplementary Fig. 3) and becomes restricted to the abaxial/ventral side of the cotyledons in heart and later stages (Fig. 2g, Supplementary Fig. 3). In *tpl-1*, *FIL* expression expands throughout the apical domain from late globular to heart stage and is subsequently

lost (Fig. 2h, Supplementary Fig. 3). *WUS* plays a critical role in SAM initiation and maintenance, and serves as a central-apical marker throughout embryogenesis18. In *tpl-1*, *WUS* is expressed correctly through the globular stage but is subsequently lost7 (Fig. 2j, k). These patterns of *FIL* and *WUS* misexpression in *tpl-1* are identical to what is seen in the triple loss-of-function mutant *rev-9 phb-6 phv-5*, and show that the apical portion of *tpl-1* embryos lose adaxial identity during the shoot to root transformation (Supplementary Fig. 4). *FIL* and *WUS* expression are restored to the WT pattern in *tpl-1 phb-14d* (Fig. 2i, l Supplementary Fig. 3). We then asked whether the loss of *HD-ZIP III* apical expression in *tpl-1* was due to expansion of *miR165/166* activity. Green Fluorescent Protein (GFP) based sensors for *miR165/166* activity, in which the sensor is inactivated in all cells where *miR165/166* are active, accumulate in a pattern similar to that of the *HD-ZIP III* mRNA and protein accumulation in the embryo (Fig. 2b, m, o, Supplementary Fig. 3, 5). Notably, the sensor is cleared from the root meristem organizing center from the globular stage on (Fig. 2m, o, Supplementary Fig. 5). If *miR165/166* were misexpressed in *tpl-1*, we would expect to observe clearance of the sensor similar to that of the mRNA of *HD-ZIP III* genes. However, the sensor continues to accumulate in the apical domain of *tpl-1* embryos grown at 29°C (Fig. 2n, p, Supplementary Fig. 5). Therefore, the loss of apical *HD-ZIP III* expression in *tpl-1* is due to a mechanism independent of *mir165/166* action and is likely at the level of transcriptional control. This represents a novel aspect of the control of *HD-ZIP III* gene expression and suggests that *HD-ZIP III* genes are excluded from the root by both transcriptional and post-transcriptional mechanisms. *miR165/166* independent loss of *HD-ZIP III* expression in *tpl-1* may be caused by *PLT1/PLT2* misexpression in apical tissues. This idea is supported by the finding that *PHB* and *REV* expression is maintained in the apical domain of *tpl-1 plt1-5 plt2-1* triple mutants (Fig. 2q, r), suggesting *PLT1/PLT2* act as negative regulators of *HD-ZIP III* expression during embryogenesis. This is also consistent with what is observed in mutants where *PHB* mRNA is thought to be completely uncoupled from *miR165/166* regulation, such as *phb1-d* and *serrate (se)*. *PHB* mRNA accumulates throughout a wide pattern in *phb1-d* and *se-5* embryos, and can lead to root defects and embryonic lethality. However, it is still restricted from the lenticular cell in these mutant backgrounds15,19 (Fig. 2f), an area of high *PLT1/PLT2* expression (Fig. 1d, f).

Double root formation in *tpl-1* requires *PLT1/PLT2* misexpression and is suppressed by GOF *HD-ZIP III* mutations. Therefore, we examined *PLT1/PLT2* gene expression in *tpl-1 phb-14d* and *tpl-1 rev-10d* double mutants grown at 29°C. *PLT1* and *PLT2* are still misexpressed in the vascular tissue and abaxial regions of developing cotyledons (Fig. 3a–d, Supplementary Fig. 4). However, we never observed *PLT* gene misexpression in the cells that would give rise to the shoot meristem. This suggests that the ability of *PLT* genes to promote root meristem formation in *tpl-1* is dependent on misexpression in the meristem, and the GOF *HD-ZIP III* alleles are able to repress the *PLT* pathway in these cells.

Our genetic studies with the GOF *HD-ZIP III* alleles and *tpl-1* implicate the *HD-ZIP III* genes in promotion of apical fate and antagonism of basal fate. *phb-6 phv-5 rev-9* triple loss-of-function mutants produce pin-shaped seedlings11 similar to what is observed at low frequency in *tpl-1*8 (Supplementary Fig. 4). *tpl-1* seedlings rarely form double roots at 24°C (2%, n=682), whereas *tpl-1 rev-9* significantly enhances the double root phenotype (48%,

n=355). Additionally, loss of *PHB* and *PHV* in the *tpl-1 rev-9* background further increases the frequency of the double-root phenotype (Table S1). At 24°C *PLT1* and *PLT2* are not broadly misexpressed in the apical domain of *tpl-1* embryos (Fig. 3e, f). However, in *tpl-1 rev-9* embryos grown at 24°C, *PLT1* and *PLT2* are misexpressed similar to *tpl-1* at 29°C (Fig. 3g, h). These results show that at lower temperatures, the *HD-ZIP III* genes act to prevent the misexpression of *PLT1/PLT2* in a *tpl-1* background.

Given that GOF *HD-ZIP III* alleles suppress *PLT1/PLT2*-dependent apical root formation in *tpl-1*, we investigated the genetic interactions of GOF *HD-ZIP III* mutants with *PLT* loss-of-function mutants. *phb-14d* and *rev-10d* have no discernible embryonic root defects (Supplementary Fig. 2) and *plt1 plt2* have only a minor defect, resulting in a properly organized seedling1. However, *phb-14d plt1-5 plt2-1* triple mutant seedlings completely lacked a root and displayed only a rudimentary hypocotyl structure (Fig. 3i, Table S2), similar to *plt1 plt2 plt3 plt4/bbm* segregants3. *rev-10d plt-5 plt2-1* seedlings showed an even more severe loss of both root and hypocotyl tissues (Fig. 3j, Table S2). In addition, *rev-10d plt1 plt2* show expansion of *REV* transcript into the root meristem region (Fig. 3k) further suggesting that the *PLT* genes play an active role in repression of the *HD-ZIP III* genes, in addition to negative regulation by *miR165/166*.

To investigate whether the *HD-ZIP III* genes could impart apical polarity to basal tissue if misexpressed in the basal pole of the early embryo, we expressed miR resistant cDNAs of the *HD-ZIP III* genes fused to the glucocorticoid receptor domain (GR) under the control of the *PLT2* promoter. When induced with dexamethasone during early embryogenesis, plants harboring either *PLT2p::REVΔmiR-GR*, *PLT2p::PHBΔmiR-GR*, or *PLT2p::ICU4ΔmiR-GR* transgenes produce seedlings that show a complete transformation of the root pole into a second shoot pole (Fig. 4a–c, Table S2, Supplementary Fig. 6).

To further characterize these homeotic transformations we examined the expression of genes specifically associated with the apical and basal poles. *PINFORMED4* (*PIN4*) is initially expressed in the embryo proper, as well as the upper cells of the suspensor (Fig. 4d). It is then restricted from the suspensor and expressed in the developing root meristem and provascular cells, and this expression has been shown to be dependent on the activity of PLT1 and PLT220 (Fig. 4e, f). In globular through heart stage *PLT2p::REVΔmiR-GR* embryos, *PIN4* mRNA is only detectable in aberrantly dividing suspensor cells (Fig. 4g, h). The loss of *PLT1/PLT2* dependant *PIN4* expression in cells ectopically expressing *REV* again illustrates the antagonistic action of these two classes of genes.

In induced globular stage *PLT2p::REVΔmiR-GR* embryos, *WUS* is misexpressed in the basal region coincident with the presumptive second shoot position, indicating that an additional shoot organizing center has formed (Fig. 4i, j). Likewise, *AINTEGUMENTA* (*ANT*) expression, which marks the cotyledon primordia in the WT21 (Fig. 4k), is misexpressed in the basal region of transition stage embryos (Fig. 4l). In older embryos, multiple basal foci of *ANT* misexpression accumulate (Fig. 4m). These results show that the alteration in embryo polarity begins during the early globular stage of induced embryos. Furthermore, these results indicate that establishment of apical fate by the *HD-ZIP III* genes precedes *WUS* and *ANT* expression (and therefore meristem and cotyledon formation).

Our results show the *HD-ZIP III* genes are master regulators of apical fate in early embryogenesis. In addition, there is a clear antagonism between the *HD-ZIP III* and *PLT* gene families, both of which are under multiple modes of regulation that ensures proper spatial distribution and apical-basal patterning (Supplementary Figure 1). Whether this antagonism is direct or is a more downstream consequence of fate change will require further investigation.

Methods Summary

Plants were grown on either soil or petri dishes containing Linsmaier and Skoog salts medium. Percival growth chambers were used for controlled temperature experiments. All other plants were grown under greenhouse conditions on a 16 hour light/8 hour dark cycle. *in situ* hybridizations were detected with digoxigenin-labeled riboprobes using the method found at http://www.its.caltech.edu/~plantlab/protocols/insitu.htm. ChIP was performed as described24 with minor modifications. The BIO-RAD MyiQ, single color, Real-Time PCR Detection System was used with the MyiQ Optical System Software for analysis of SYBR Green I stained amplification products. Embryos were cleared with Hoyer's solution and DIC images were collected using a Leica DM5000B microscope. Confocal images were collected using a Leica DM IRE2 laser scanning confocal microscope.

Materials and Methods

Plant growth and mutant alleles

Plants were grown on either soil or petri dishes containing Linsmaier and Skoog salts medium. Percival growth chambers were used for controlled temperature experiments. All other plants were grown under greenhouse conditions on a 16 hour light/8 hour dark cycle. All mutants, with the exception of *icu4-1d* are in the Landsberg erecta (Ler) ecotype. Germplasm used were as follows: *plt1-5* and *plt2-1*1, *rev-10d*11, *phb-1d*16, *phb-6 phv-5 rev-9*11, *icu4-1d*13. *icu4-1d* was isolated in the Enkheim-2 (En-2) and back crossed to *tpl-1* four times.

In situ hybridization

In situ hybridizations were detected with digoxigenin-labelled riboprobes using the method found at http://www.its.caltech.edu/~plantlab/protocols/insitu.htm. *PHB, PHV, REV*, and *FIL*, probes were made generated using 300–700bp regions of coding sequence using the primers listed in Supplementary Table 3. *PLT1, PLT2, ICU4, WUS, ANT, PIN4* and *GFP* probes were generated using full length cDNAs.

Chromatin Immunoprecipitation

ChIP was performed as described22 with the following modifications. Ovules were dissected from siliques containing globular to heart stage embryos. Tissue was fixed in 2% formaldehyde/PBS under vacuum for 2 hrs, replacing vacuum every 30 min. 500mg of starting material was used for each ChIP sample. The anti-HA monoclonal antibody HA.11 (Covance) and M-280 sheep anti-mouse IgG Dynabeads (Invitrogen) were used to

immunoprecipitate TPL-HA fusion. Two negative controls were performed, including a no antibody sample and a ChIP reaction performed on wild type (no transgene) tissue.

Real-time PCR

The BIO-RAD MyiQ, single color, Real-Time PCR Detection System was used with the MyiQ Optical System Software for analysis. SYBR Green I was used as an intercalating fluorescent dye. The standard curve method was used to determine reaction efficiency for each primer pair and determine fold enrichment by comparing the CT (threshold cycle) values of IP and negative control which were normalized normalize by calculating input(IP)/ input(control) when appropriate.

Plasmid Construction

The miR165/166 sensor was generated using complementary 42 base pair primers encompassing the miR165/166 recognition sequence in *PHB* and *REV*, which were annealed to generate double stranded fragments with EcoRI compatible sites at each end. These fragments were then treated with T4 polynucleotide kinase in T4 DNA ligase buffer and cloned into a unique EcoRI site in the mERGFP5 sequence that lies between the endoplasmic reticulum (ER) localization signal and mGFP5. The modified mERGFP5 were then cloned as a BamHI fragments into a pBJ36 construct, 3’ to a 925bp promoter fragment from the potato UBI3 gene23. For the negative control, three silent mutations were introduced within the 3’ end of the miR recognition sequence. Primers used are listed in Supplementary Table 3.

For construction of the *PLT2p::HD-ZIPIII-GR* constructs, a 4380 bp genomic fragment 5’ to the *PLT2* start codon was cloned as a XhoI/SalI fragment into a SalI site of a pBJ36 vector containing the hormone binding domain of the rat glucocorticoid receptor24. *HD-ZIP III* miR resistant cDNAs were generated by inducing three silent mutations within the 3’ end of the miR recognition sequence by site directed mutagenesis using the primers listed in Supplementary Table 3.

Microscopy

Excised ovules were mounted in Hoyer’s solution for analysis of embryonic morphology. Embryos were imaged using a Leica DM5000B microscope, seedlings using a Leica MZ FLIII microscope. For GFP analysis, ovules were dissected into 0.5X LS media (Caisson Laboratories, Inc.; Rexburg, ID), vacuum infiltrated in 4% paraformaldehyde, rinsed with water, vacuum infiltrated with 2% SCRI Renaissance 2200 (Renaissance Chemicals Ltd.; North Yorkshire, UK) and 4% DMSO, then washed 2X and mounted in 20% glycerol. Embryos were imaged using a Leica DM IRE2 laser scanning confocal microscope. SR2200 was excited with the UV diode 405nm line, and emission was measured between at 420–470nm. GFP was excited with a 488nm argon laser line and emission was measured at 500–535nm.

Supplementary Material

Refer to Web version on PubMed Central for supplementary material.

Acknowledgements

We thank J. Sewell for technical assistance with plasmid construction and microscopy; R. Biddick, B. Crawford, D.B. Jaillais, N. Krogan, J. Posakony, B. VanSchooten, and D. Kelley for critical discussions and reading of the manuscript; E. York and SIO Unified Laboratory Facility for SEM analysis; This work was supported by a Ray Thomas Edwards Foundation Career Development Award, the National Institute of Health, NIGMS (J.A.L.), Z.R.S. is a USCD Plant Systems Biology NSF-IGERT Fellow.

References

1. Aida M, et al. The PLETHORA genes mediate patterning of the Arabidopsis root stem cell niche. Cell. 2004; 119(1):109–120. [PubMed: 15454085]
2. Blilou I, et al. The PIN auxin efflux facilitator network controls growth and patterning in Arabidopsis roots. Nature. 2005; 433(7021):39–44. [PubMed: 15635403]
3. Galinha C, et al. PLETHORA proteins as dose-dependent master regulators of Arabidopsis root development. Nature. 2007; 449(7165):1053–1057. [PubMed: 17960244]
4. Friml J, et al. Efflux-dependent auxin gradients establish the apical-basal axis of Arabidopsis. Nature. 2003; 426(6963):147–153. [PubMed: 14614497]
5. Gray WM, Kepinski S, Rouse D, Leyser O, Estelle M. Auxin regulates SCF(TIR1)- dependent degradation of AUX/IAA proteins. Nature. 2001; 414(6861):271–276. [PubMed: 11713520]
6. Szemenyei H, Hannon M, Long J. TOPLESS mediates auxin dependent transcriptional repression during Arabidopsis embryogenesis. Science. 2008 In Press.
7. Long JA, Ohno C, Smith ZR, Meyerowitz EM. TOPLESS regulates apical embryonic fate in Arabidopsis. Science. 2006; 312(5779):1520–1523. [PubMed: 16763149]
8. Long JA, Woody S, Poethig S, Meyerowitz EM, Barton MK. Transformation of shoots into roots in Arabidopsis embryos mutant at the TOPLESS locus. Development. 2002; 129(12):2797–2806. [PubMed: 12050130]
9. Tang G, Reinhart BJ, Bartel DP, Zamore PD. A biochemical framework for RNA silencing in plants. Genes Dev. 2003; 17(1):49–63. [PubMed: 12514099]
10. Mallory AC, et al. MicroRNA control of PHABULOSA in leaf development: importance of pairing to the microRNA 5' region. Embo J. 2004; 23(16):3356–3364. [PubMed: 15282547]
11. Emery JF, et al. Radial patterning of Arabidopsis shoots by class III HD-ZIP and KANADI genes. Curr Biol. 2003; 13(20):1768–1774. [PubMed: 14561401]
12. Floyd SK, Bowman JL. Gene regulation: ancient microRNA target sequences in plants. Nature. 2004; 428(6982):485–486. [PubMed: 15057819]
13. Ochando I, et al. Mutations in the microRNA complementarity site of the INCURVATA4 gene perturb meristem function and adaxialize lateral organs in arabidopsis. Plant Physiol. 2006; 141(2):607–619. [PubMed: 16617092]
14. Zhong R, Taylor JJ, Ye ZH. Transformation of the collateral vascular bundles into amphivasal vascular bundles in an Arabidopsis mutant. Plant Physiol. 1999; 120(1):53–64. [PubMed: 10318683]
15. McConnell JR, et al. Role of PHABULOSA and PHAVOLUTA in determining radial patterning in shoots. Nature. 2001; 411(6838):709–713. [PubMed: 11395776]
16. McConnell JR, Barton MK. Leaf polarity and meristem formation in Arabidopsis. Development. 1998; 125(15):2935–2942. [PubMed: 9655815]
17. Prigge MJ, et al. Class III homeodomain-leucine zipper gene family members have overlapping, antagonistic, and distinct roles in Arabidopsis development. Plant Cell. 2005; 17(1):61–76. [PubMed: 15598805]
18. Mayer KF, et al. Role of WUSCHEL in regulating stem cell fate in the Arabidopsis shoot meristem. Cell. 1998; 95(6):805–815. [PubMed: 9865698]
19. Grigg SP, et al. Repression of Apical Homeobox Genes Is Required for Embryonic Root Development in Arabidopsis. Curr Biol. 2009
20. Friml J, et al. AtPIN4 mediates sink-driven auxin gradients and root patterning in Arabidopsis. Cell. 2002; 108(5):661–673. [PubMed: 11893337]

21. Elliott RC, et al. AINTEGUMENTA, an APETALA2-like gene of Arabidopsis with pleiotropic roles in ovule development and floral organ growth. Plant Cell. 1996; 8(2):155–168. [PubMed: 8742707]

22. Bowler C, et al. Chromatin techniques for plant cells. Plant J. 2004; 39(5):776–789. [PubMed: 15315638]

23. Garbarino JE, Belknap WR. Isolation of a ubiquitin-ribosomal protein gene (ubi3) from potato and expression of its promoter in transgenic plants. Plant Mol Biol. 1994; 24(1):119–127. [PubMed: 8111011]

24. Aoyama T, Chua NH. A glucocorticoid-mediated transcriptional induction system in transgenic plants. Plant J. 1997; 11(3):605–612. [PubMed: 9107046]

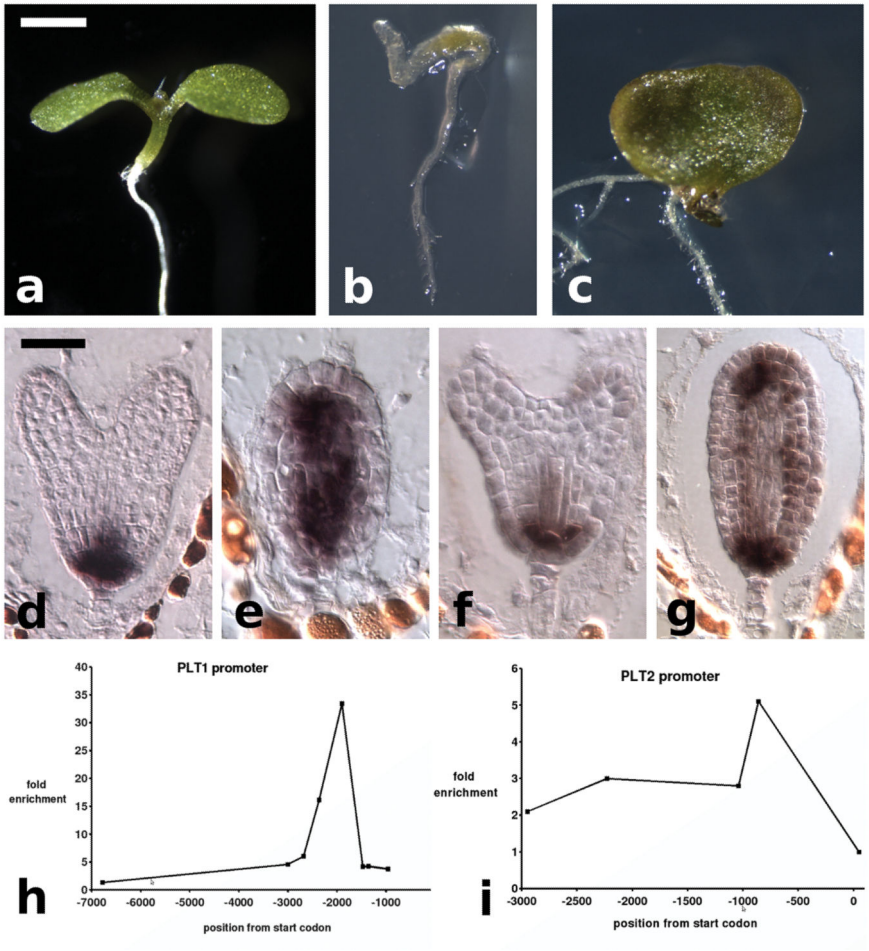

Figure 1. Misregulation of *PLT* genes is necessary for *tpl-1* apical to basal transformation

a–c, Seedlings from embryos grown at 29°C. **a**, WT seedling. **b**, *tpl-1* double root. **c**, *tpl-1 plt1-5 plt2-1* monocot. **d–g** *in situ* hybridization with *PLT1* and *PLT2* antisense probe, embryos grown at 29°C. **d**, *PLT1* expression in WT. **e**, *PLT1* expression in *tpl-1*. **f**, *PLT2* expression in WT. **g**, *PLT2* expression in *tpl-1*. **h**, graph of fold enrichment at the *PLT1* locus from ChIP of TPLp::TPL-HA. **i**, graph of fold enrichment at the *PLT2* locus from ChIP of TPLp::TPL-HA. Scale bars, 1 mm (**a–c**) and 50 μm (**d–g**).

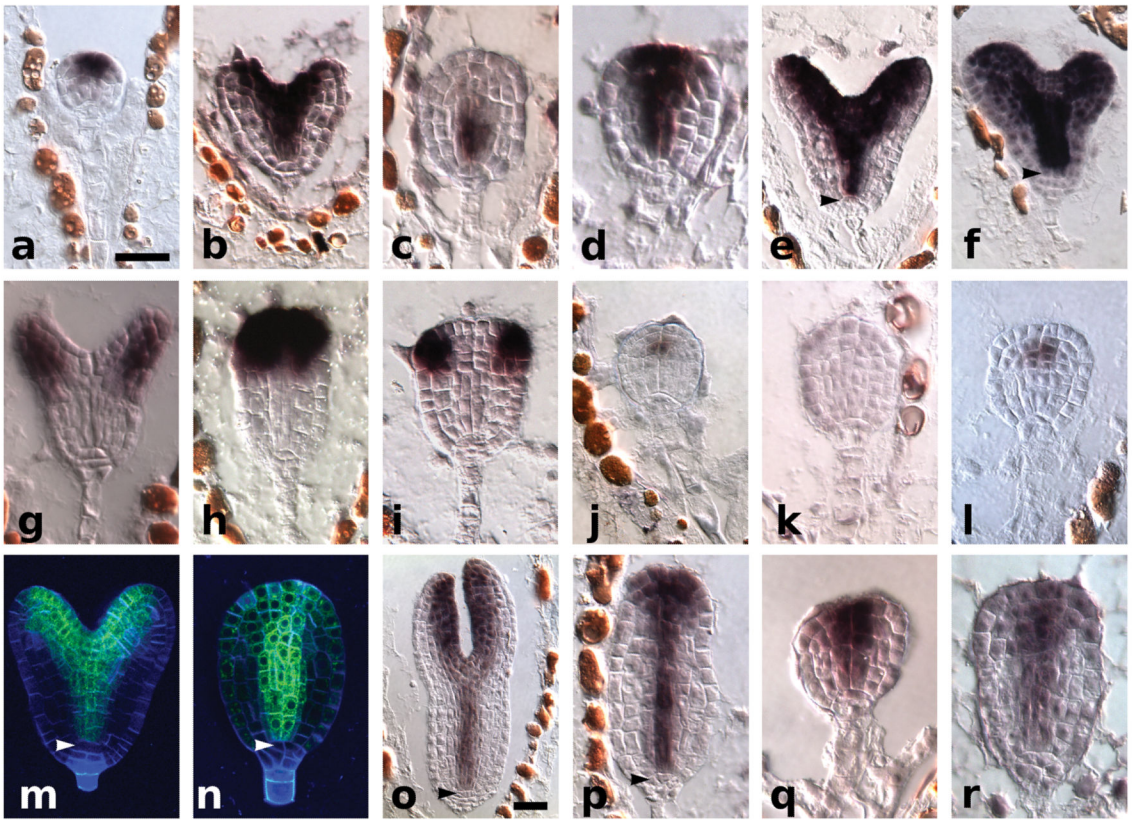

Figure 2. Molecular characterization of *tpl-1*, *phb-14d*, and *tpl-1 phb-14d* in embryos grown at 29°C

a–f, *PHB in situ* hybridizations. WT globular (**a**) and early heart (**b**) stage, *tpl-1* transition stage (**c**), *tpl-1 phb-14d* transition stage (**d**), *phb-14d* heart stage (**e**), and *phb-1d* heart stage (**f**). **g–i**, *FIL in situ* hybridizations. WT (**g**), *tpl-1* (**h**), and *tpl-1 phb-14d* (**i**). **j–l**, *WUS in situ* hybridizations. WT (**j**), *tpl-1* (**k**), and *tpl-1 phb-14d*. (**l**). **m–p**, miR165/166 sensor. GFP fluorescence in WT (**m**) and *tpl-1* (**n**). *GFP in situ* hybridizations in WT (**o**) and *tpl-1* (**p**). **q**, *PHB in situ* hybridizations in *tpl-1 plt1-5 plt2-1*. **r**, *REV in situ* hybridization in *tpl-1 plt1-5 plt2-1*. Arrowheads indicate the root meristem organizing center. Scale bars, 50 μm (**a–r**).

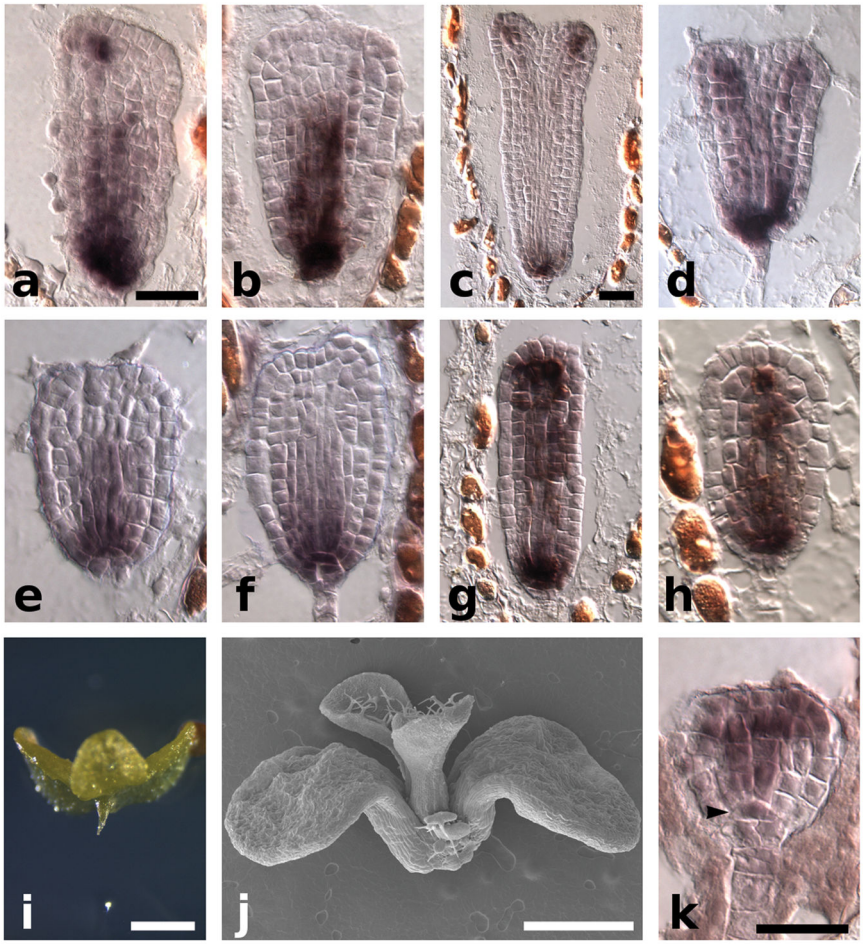

Figure 3. *HD-ZIP III* genes antagonize *PLT* function

a–c, *in situ* hybridizations with *PLT1*/*PLT2* in 29°C grown embryos. **a**, *PLT1* in *tpl-1 phb-14d*. **b**, *PLT1* in *tpl-1 rev- 10d*. **c**, *PLT2* in *tpl-1 phb-14d*. **d**, *PLT2* in *tpl-1 rev-10d*. **e–h**, *PLT1/PLT2 in situ* hybridizations in 24°C grown embryos. **e**, *PLT1* in *tpl-1*. **f**, *PLT2* in *tpl-1*. **g**, *PLT1* in *tpl-1 rev-9*. **h**, *PLT2* in *tpl-1 rev-9*. **i**, *phb-14d plt1-5 plt2-1* seedling. **j**, Scanning electron micrograph (SEM) of *rev-10d plt1-5 plt2-1* seedling. **k**, *REV in situ* hybridization in *rev-10d plt1-2 plt2-1*. Scale bars, 50 μm (**a–h, k**) and 1 mm (**i, j**).

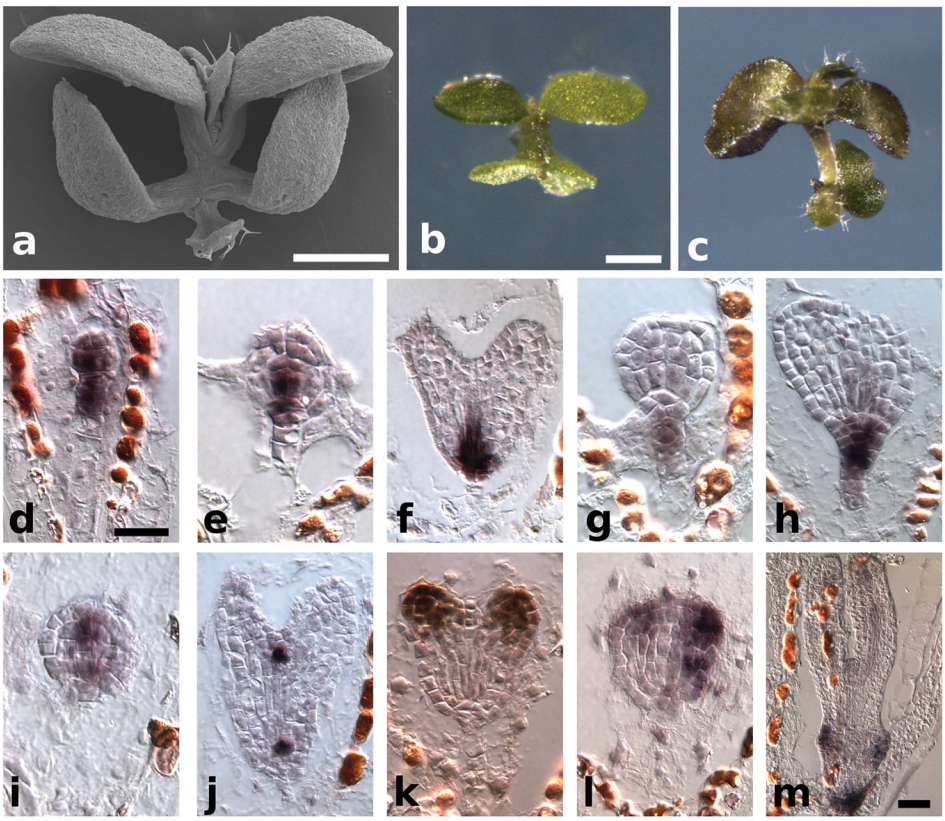

Figure 4. *HD-ZIP III* gene misexpression can initiate apical fate and acts antagonistically to *PLT* gene function

a, SEM image of *PLT2p:REVΔmiR-GR* seedling. **b**, *PLT2p:PHBΔmiR-GR* seedling. **c**, *PLT2p::ICU4ΔmiR-GR* seedling. **d–h**, *in situ* hybridizations with anti-sense *PIN4* probe. **d–f**, WT 16-cell (**d**), globular (**e**), and heart (**f**) stage. **g–h**, *PLT2p:REVΔmiR-GR* globular stage (**g**) and late heart stage (**h**) embryos after dexamethasone induction. **i–j**, *in situ* hybridizations with anti-sense *WUS* probe in *PLT2p:REVΔmiR-GR* globular (**i**) and heart (**j**) stage embryos after induction. **k–m**, *in situ* hybridizations with anti-sense *ANT* probe in WT transition stage (**k**) and *PLT2p:REVΔmiR-GR* transition stage (**l**) and torpedo stage (**m**) embryos after induction. Scale bars, 1 mm (**a–c**) and 50 μm (**d–m**).

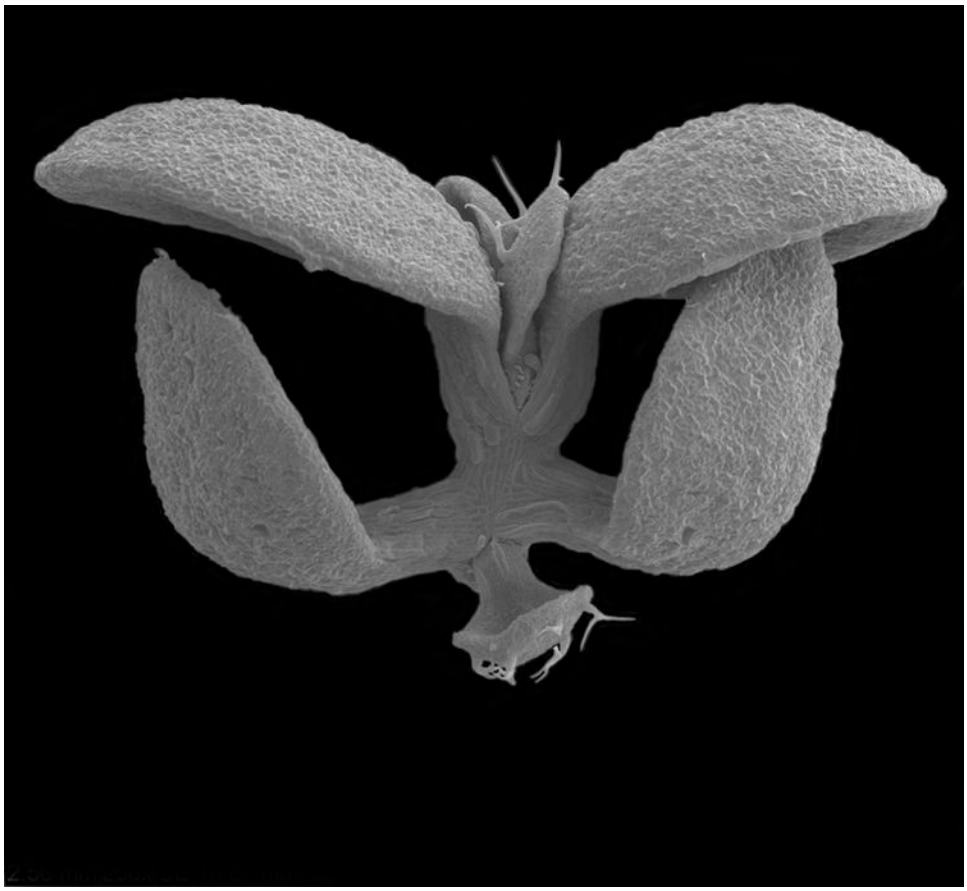

Figure 5.

Figure 6.